Обзор ArXiv/astro-ph, 8-13 апреля 2022

От Сильченко О.К.

ArXiv: 2204.02989

BIRTH OF THE GALACTIC DISK REVEALED BY THE H3 SURVEY

CHARLIE CONROY[1], DAVID H. WEINBERG[2], ROHAN P. NAIDU[1], TOBIAS BUCK[3], JAMES W. JOHNSON[2], PHILLIP CARGILE[1], ANA BONACA[4], NELSON CALDWELL[1], VEDANT CHANDRA[1], JIWON JESSE HAN[1], BENJAMIN D. JOHNSON[1], JOSHUA S. SPEAGLE (沈佳士)[5,6,7,8], YUAN-SEN TING (丁源森)[9,10], TURNER WOODY[1], DENNIS ZARITSKY[11]

Submitted to ApJ

ABSTRACT

We use chemistry ([α/Fe] and [Fe/H]), main sequence turnoff ages, and kinematics determined from H3 Survey spectroscopy and *Gaia* astrometry to identify the birth of the Galactic disk. We separate in-situ and accreted stars on the basis of angular momenta and eccentricities. The sequence of high–α in-situ stars persists down to at least [Fe/H] ≈ -2.5 and shows unexpected non-monotonic behavior: with increasing metallicity the population first declines in [α/Fe], then increases over the range $-1.3 \lesssim$ [Fe/H] $\lesssim -0.7$, and then declines again at higher metallicities. The number of stars in the in-situ population rapidly increases above [Fe/H] ≈ -1. The average kinematics of these stars are hot and independent of metallicity at [Fe/H] $\lesssim -1$ and then become increasingly cold and disk-like at higher metallicities. The ages of the in-situ, high–α stars are uniformly very old (≈ 13 Gyr) at [Fe/H] $\lesssim -1.3$, and span a wider range ($8-12$ Gyr) at higher metallicities. Interpreting the chemistry with a simple chemical evolution model suggests that the non-monotonic behavior is due to a significant increase in star formation efficiency, which began ≈ 13 Gyr ago. These results support a picture in which the first ≈ 1 Gyr of the Galaxy was characterized by a "simmering phase" in which the star formation efficiency was low and the kinematics had substantial disorder with some net rotation. The disk then underwent a dramatic transformation to a "boiling phase", in which the star formation efficiency increased substantially, the kinematics became disk-like, and the number of stars formed increased tenfold. We interpret this transformation as the birth of the Galactic disk at $z \approx 4$. The physical origin of this transformation is unclear and does not seem to be reproduced in current galaxy formation models.

Данные

2. DATA

In this paper we use data from the H3 Stellar Spectroscopic Survey (Conroy et al. 2019) and *Gaia* EDR3 (Gaia Collaboration et al. 2021). H3 is collecting $R = 32,000$ spectra over the wavelength range 5150Å–5300Å using the Hectochelle spectrograph on the MMT telescope (Fabricant et al. 2005; Szentgyorgyi et al. 2011). The survey will eventually collect 300,000 spectra over $\approx$ 1500 uniformly spaced fields covering $|b| > 20°$ and Dec. $> -20°$. As of March 2022 the survey has collected 208,000 spectra over 1,100 fields. The primary survey selection function is based solely on magnitude ($15 < r < 18$) and *Gaia* parallax (a selection that has evolved from $\pi < 0.5$ mas to $\pi < 0.3$ mas as the *Gaia* data quality has improved). The survey includes additional rare high-value targets and filler targets that are both fainter and at higher parallax than the main sample. The high parallax filler sample constitutes $\approx 60\%$ of the sample used below.

Stellar parameters are derived using the `MINESweeper` program (Cargile et al. 2020). `MINESweeper` simultaneously fits the high-resolution spectrum and the broadband photometry (from SDSS, Pan-STARRS, *Gaia*, 2MASS, *WISE*) to a library of synthetic spectral grids and isochrones. Derived parameters include radial velocities, distances, reddening, rotational line broadening, $V_{\rm rot}$, [Fe/H], and [α/Fe]. In the model fit-

In this paper we focus on a high-quality subset of the H3 data. In particular, we require spectroscopic SNR > 20, log $g > 3.5$, $V_{\rm rot} < 2$ km s^{-1}, *Gaia* RUWE < 1.5, and $\chi^2_{\rm spec}$/DOF < 2.5. There are a variety of data quality flags; we require that no flags have been set. The SNR, flag, and log g cuts reduce the sample to 9,476 stars. The RUWE cut reduces the sample to 9,163 stars, and the last two cuts result in a final sample of 8,544 stars. For this sample, the median SNR of the *Gaia* EDR3 parallax and proper motion is 17 and > 100, respectively. The median formal uncertainties on [Fe/H] and [α/Fe] are 0.02, although they increase toward lower metallicities such that the median uncertainties are 0.05 at [Fe/H] $= -2$.

Owing to the parallax selection of the overall survey com-

|Z|>0.7 kpc, max 1.3 kpc

Разделение на собственные и приобретенные звезды

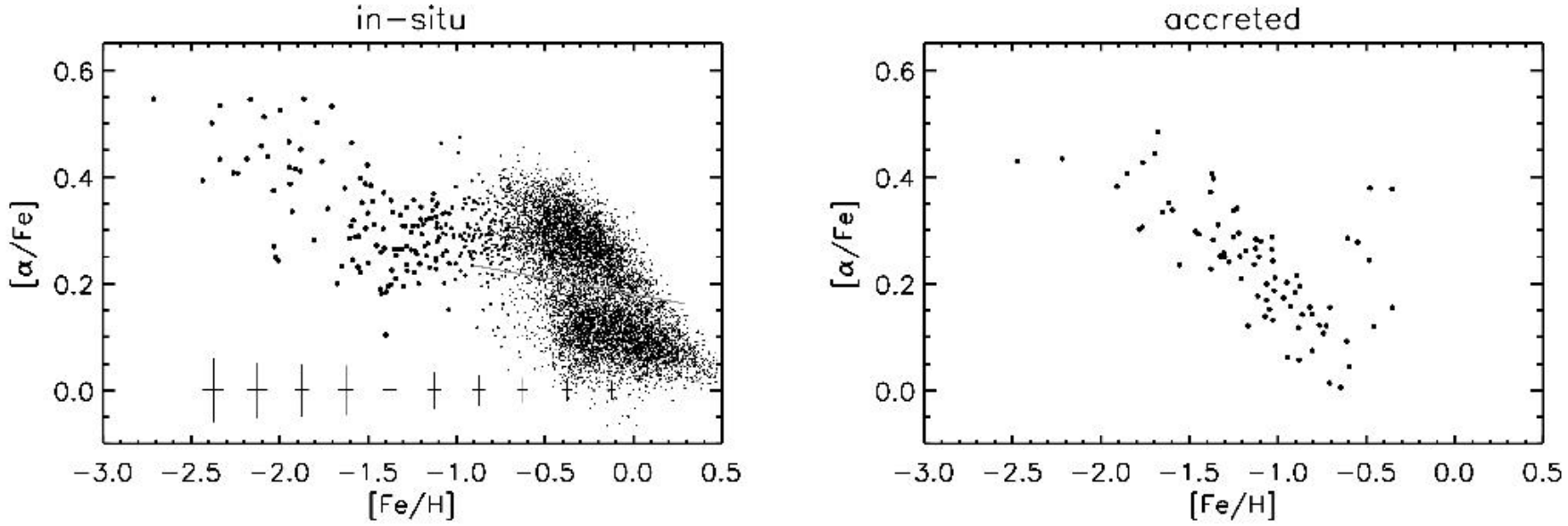

Figure 1. Chemistry of in-situ and accreted stars from the H3 Survey. In-situ stars are defined to have prograde orbits ($L_Z < 0$) with eccentricities $e < 0.8$, while accreted stars are defined to have $e > 0.9$ or a combination of $e > 0.8$ and $L_Z > 500$ km s^{-1} kpc^{-1} (retrograde orbits). In the left panel, one clearly sees the high−α and low−α sequences at [Fe/H] $\gtrsim -0.7$. Moving to lower metallicities the high−α population declines in [α/Fe] until [Fe/H] ≈ -1.3, at which point [α/Fe] increases. The grey line highlights our adopted separation between high−α and low−α populations. The accreted population (right panel) displays a linear decline in [α/Fe] with increasing metallicity. The ≈ 7 outlier stars at [Fe/H] $\gtrsim -0.5$ are likely heated stars from the in-situ population. In the left panel, symbol size is inversely proportional to metallicity in order to draw attention to the low-metallicity sequence, and the average uncertainties are shown as a function of metallicity along the bottom.

Полный диапазон металличностей

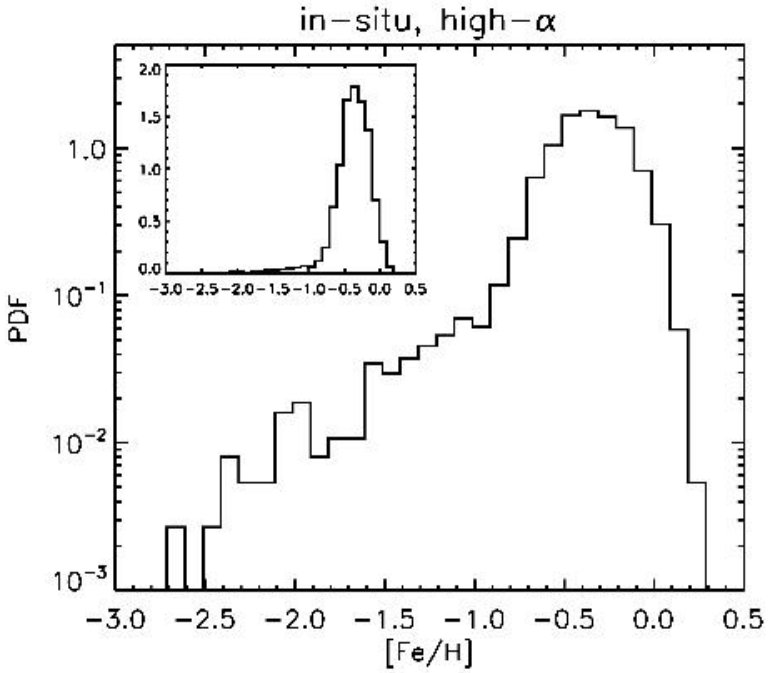

Figure 2. Metallicity distribution function (MDF) of the in-situ, high−α population. The inset shows the MDF on a linear scale. There is a substantial increase in stars above a metallicity of [Fe/H] ≈ -1.0.

Металличный толстый диск – динамически холодный

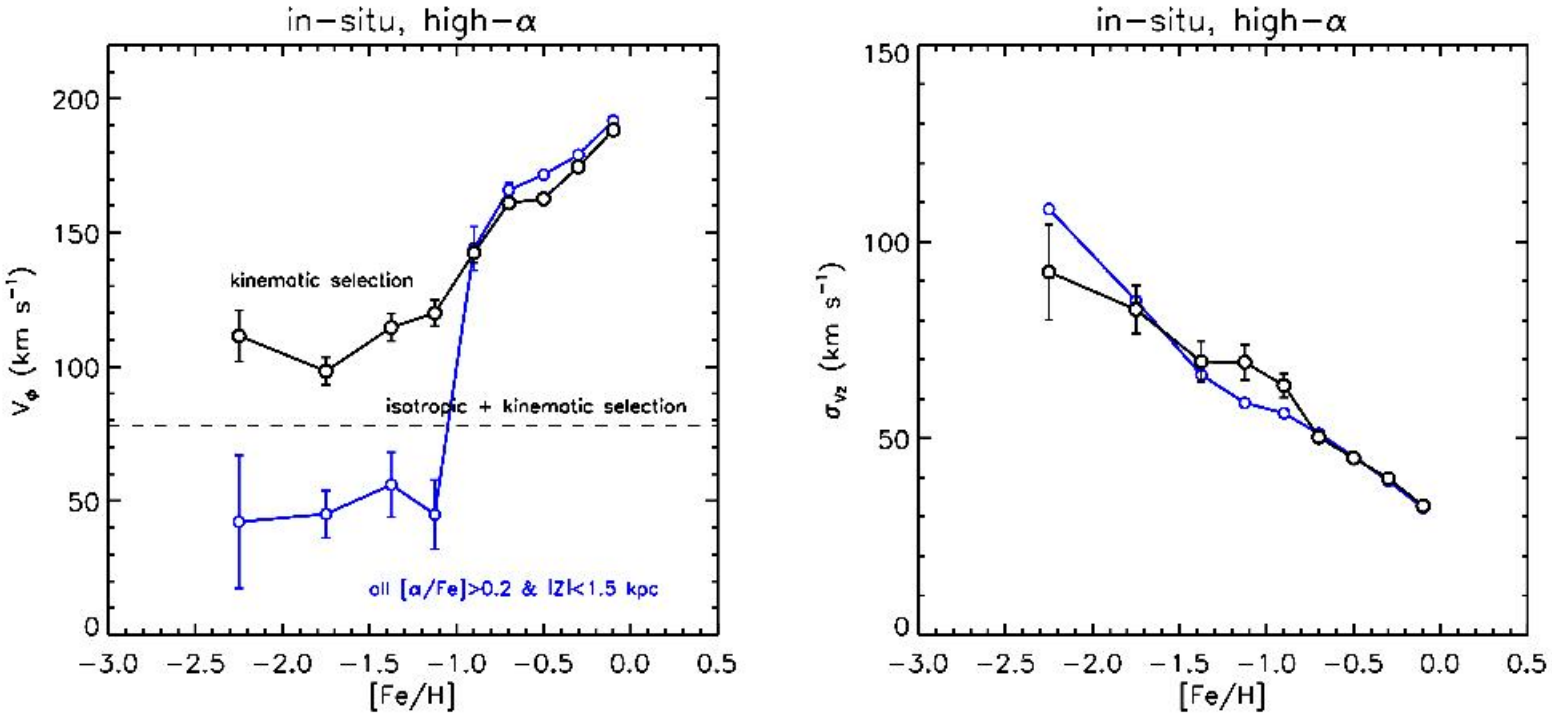

Figure 3. Average kinematic behavior of the in-situ, high−α population as a function of metallicity. Left panel: average azimuthal velocity (V_ϕ). Right panel: vertical velocity dispersion (σ_{V_z}). Our kinematic selection of the in-situ sample (black line) is compared to a sample selected only to have high α and $|Z| < 1.5$ kpc (blue line). The former selection will bias the azimuthal velocity high because stars on retrograde and radial orbits are removed, while the latter will bias the velocity low because some accreted stars, which have preferentially radial orbits, are included. The true azimuthal velocity of the in-situ population lies in between the black and blue lines. Below a metallicity of [Fe/H] ≈ -1 the population is kinematically hot with little net rotation; at higher metallicities the population is increasingly cold and disk-like. We include in the left panel a dashed line that indicates the average value for an intrinsically isotropic velocity distribution with the in-situ sample selection applied.

Напрямую (по изохронам) померянные возраста звезд

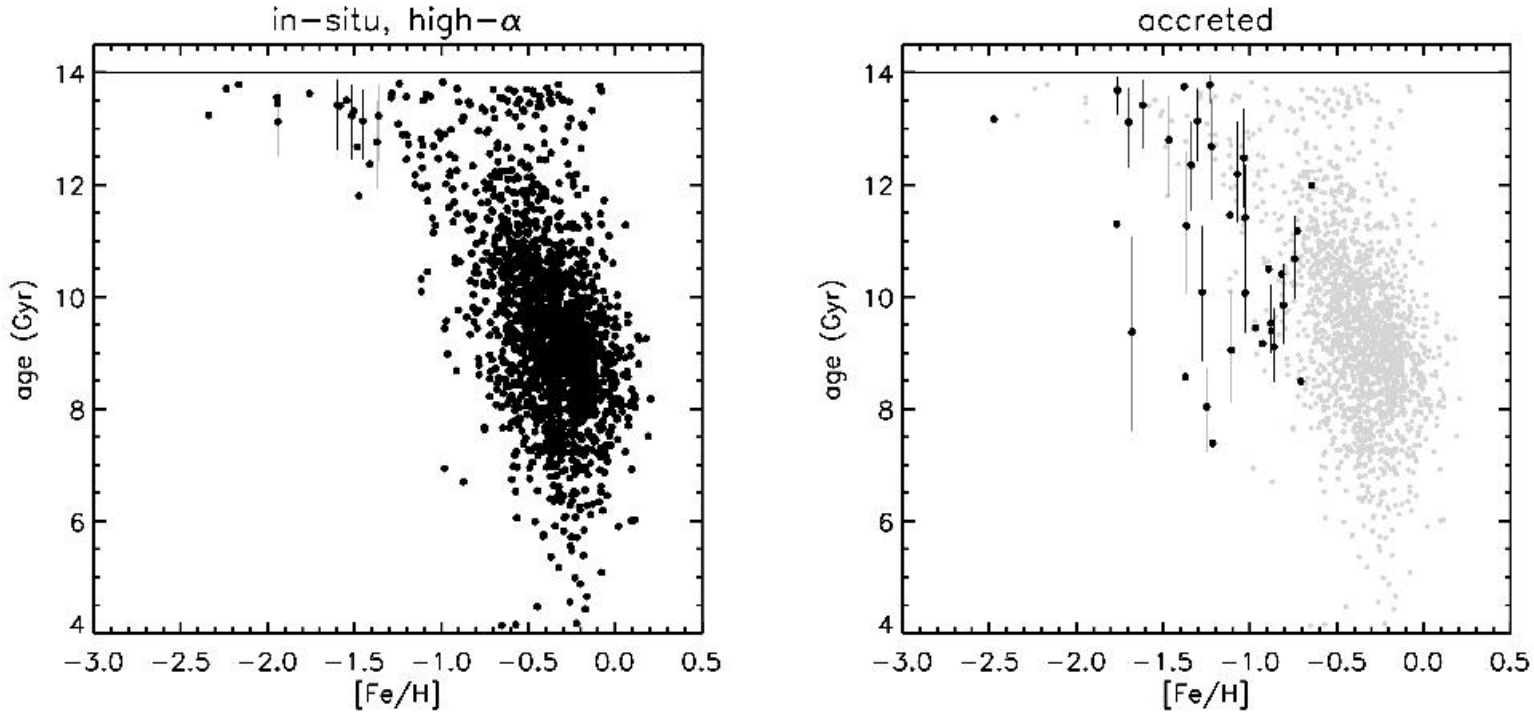

Figure 4. Ages of the in-situ, high−α (left panel) and accreted (right panel) stars as a function of metallicity. The sample here is restricted to main sequence turnoff and subgiant stars ($3.8 < \log g < 4.2$) where age estimates are most reliable. The upper limit on allowed ages is 14 Gyr (solid line). Error bars represent formal 68% confidence intervals; in the left panel they are shown only at [Fe/H] < -1.3 for clarity. In the right panel, the in-situ stars are shown as light grey points for direct comparison. The in-situ, high−α population is uniformly very old at [Fe/H] $\lesssim -1.3$, with ages $\gtrsim$ 12 Gyr. At metallicities above [Fe/H] ≈ -1 the ages span a wide range, from $\approx 8-12$ Gyr. In contrast to the in-situ population, the accreted population contains stars younger than 12 Gyr even at low metallicities.

Модель химической эволюции

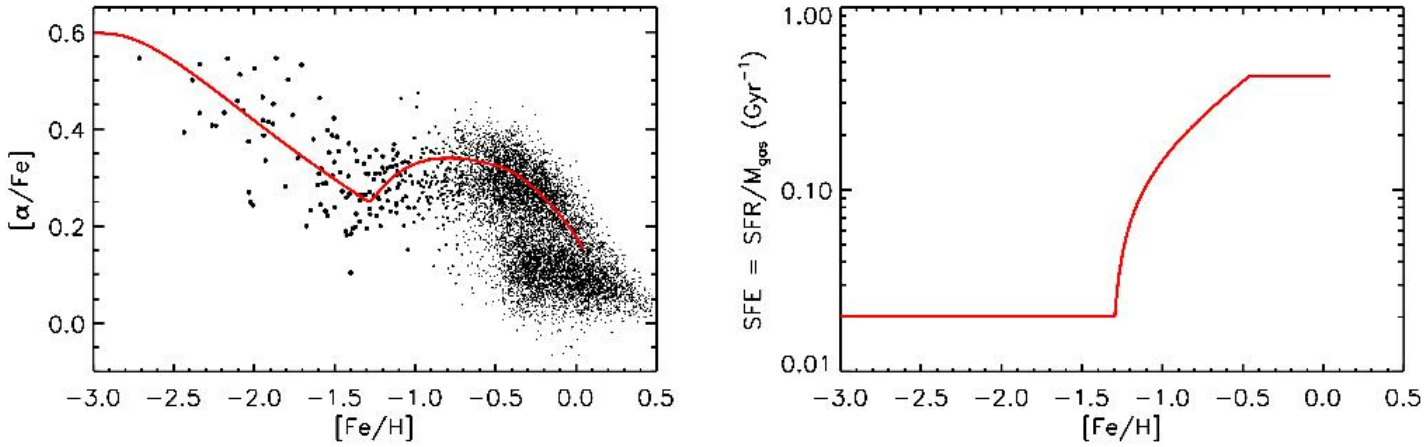

Figure 5. Chemical evolution modeling of the in-situ, high−α population. The red line shows a simple model in which the SFR is related to the gas mass by the star formation efficiency, whose behavior is shown in the right panel. The model has a constant gas inflow rate and a mass-loading factor $\eta \equiv \dot{M}_{\rm out}/{\rm SFR} = 2$. The key point is that the change in chemical evolution track around [Fe/H] ≈ -1.3 is driven by a large increase in the star formation efficiency.

[Fe/H] = −1.3. We interpret the rise in [α/Fe] between [Fe/H] = −1.3 and −0.7 as a consequence of accelerating star formation, which increases the rate of CC enrichment relative to Ia enrichment. To achieve a good fit to the observed trend, we adopt the following functional form for τ_* (in units of Gyr):

$$\tau_* = \begin{cases} 50 & t < 2.5\,{\rm Gyr} \\ 50/[1+3(t-2.5)]^2 & 2.5 \le t \le 3.7\,{\rm Gyr} \\ 2.36 & t > 3.7\,{\rm Gyr}. \end{cases} \quad (3)$$

An instantaneous decrease in τ_* at 2.5 Gyr would result in a rapid increase in [Mg/Fe] at nearly fixed [Fe/H] (see below, and Weinberg et al. 2017; Johnson & Weinberg 2020). In order to match the observations we required a more gradual change; the precise function was determined by trial-and-error.

Сценарий формирования Млечного Пути

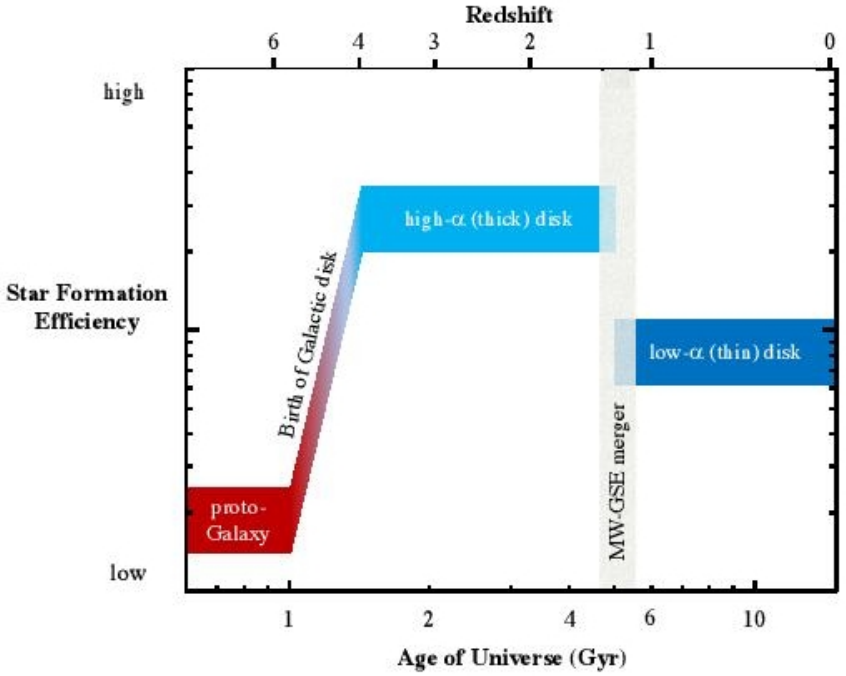

Figure 8. Schematic overview of Galactic star formation efficiency (SFE) over cosmic time. The colors indicate the kinematic state of the forming component (red = hot, blue = cold). At early times the proto-Galaxy has low SFE and is kinematically hot. After a period of $\sim$ 1 Gyr, the SFE rapidly increases and the kinematics become much colder. This marks the beginning of the high–α (thick) disk phase. At $z \sim 1$ the GSE finishes merging with the Galaxy. This event truncates the high–α disk, creates the in-situ halo via kicked up high–α disk stars, and initiates the epoch of low–α (thin) disk formation. In this final phase, the kinematics are colder and the SFE lower than the high–α disk (Nidever et al. 2014). Epochs are approximate. See text for details.

Выводы

- Считают, что НАБЛЮДАТЕЛЬНО установлено резкое увеличение эффективности звездообразования в Млечном Пути на z=4, приведшее к началу формирования диска.
- ЭТОТ диск стал толстым после слияния с Сосиской-Энцеладом 8 млрд лет назад
- Причина резкого начала SF на z=4 пока непонятна; в космологических моделях похожие явления связаны с мержингом, но случаются исключительно на z<1 (NIHAO)